UDC 544.2/.7:544.22 DOI https://doi.org/10.35546/kntu2078-4481.2024.4.6

I. V. KOVINCHUK
Postgraduate Student at the Department of Physical Chemistry
National Technical University of Ukraine
"Igor Sikorsky Kyiv Polytechnic Institute",
University of Palermo, Palermo, Italy
ORCID: 0000-0003-4841-992X

G. LAZZARA
Doctor of Chemical Sciences,
Professor at the Department of Chemistry and Physics
University of Palermo, Palermo, Italy
ORCID: 0000-0003-1953-5817

A. V. RAGULYA
Doctor of Technical Sciences, Professor,
Head of the Department of Physics, Chemistry
and Technology of Nanostructured Ceramics and Nanocomposites
Frantsevich Institute for Problems of Materials Science
National Academy of Science of Ukraine
ORCID: 0000-0002-0859-0004

M. M. KRŽMANC
Doctor of Chemical Sciences,
Senior Researcher at the Advanced Materials Department
Jožef Stefan Institute, Ljubljana, Slovenia
ORCID: 0000-0003-3436-5692

G. V. SOKOLSKY
Doctor of Chemical Sciences, Professor,
Professor at the Department of Physical Chemistry
National Technical University of Ukraine
"Igor Sikorsky Kyiv Polytechnic Institute"
ORCID: 0000-0002-6665-2744

EVALUATION OF NANOPARTICLES' SIZE CHARACTERISTICS OF MANGANESE OXIDE/HYDROXIDE BASED PHOTOCATALYSTS

Since size is a key characteristic determining whether a material belongs to the nanomaterial class, its accurate assessment is critical. In addition, the size effect in nanoparticles defines the efficiency of the material for catalytic and photocatalytic applications. A series of composite materials composed of manganese oxide/hydroxide compounds with halloysite nanotubes were synthesized and characterized, with a focus on nanoparticles size parameters critical for functional applications. Multiple analytical techniques, including transmission and scanning electron microscopy (TEM/SEM) combined with IMAGJ software, dynamic light scattering (DLS), and X-ray diffraction (XRD), were employed to evaluate sizes of nanoparticles. Samples were chemically synthesized at ambient temperature of 15–20°C from a solution of $MnSO_4$ with H_2O_2 as an oxidising agent at different pH. The size distribution half-width was identified as a key factor in estimating the error associated with size effects in nanomaterials. It can be seen that the relative error towards even critical for quantum effects revealing size of 100 nm makes up about 10% for synthesized samples and about 20% for standard MnO_2 from Pridneprovsky Chemical Plant (Ukraine). These error values are large enough for quantitative evaluations and highlight the need for improved control over size distribution through optimized synthesis conditions, in particular, temperature. Furthermore, while XRD primarily reflects the sizes of crystallites, often smaller than the actual nanoparticles' sizes observed via TEM/SEM, DLS tends to overestimate sizes due to particle agglomeration. From the analysis of nanoparticle size data of studied Samples, the Rietveld refinement resulted in good agreement with IMAGJ software data for particular cases of Samples taken for analysis. The comprehensive characterization of the samples underscores their potential for future nanoapplications, providing a foundation for further research and development.

Key words: *nanoparticle, size, evaluation, manganese oxides/hydroxides, photocatalysis.*

І. В. КОВІНЧУК
аспірантка кафедри фізичної хімії
Національний технічний університет України
«Київський політехнічний інститут імені Ігоря Сікорського»,
Університет Палермо, Палермо, Італія
ORCID: 0000-0003-4841-992X

Д. ЛАЗЗАРА
доктор хімічних наук, професор кафедри хімії та фізики
Університет Палермо, Палермо, Італія
ORCID: 0000-0003-1953-5817

А. В. РАГУЛЯ
доктор технічних наук, професор,
завідувач відділу фізики, хімії
та технології наноструктурної кераміки та нанокомпозитів
Інститут проблем матеріалознавства імені Францевича
Національної академії наук України
ORCID: 0000-0002-0859-0004

М. М. КРЖМАНЦ
доктор хімічних наук,
старший науковий співробітник відділення перспективних матеріалів
Інститут Йожефа Стефана, Любляна, Словенія
ORCID: 0000-0003-3436-5692

Г. В. СОКОЛЬСЬКИЙ
доктор хімічних наук, професор,
професор кафедри фізичної хімії
Національний технічний університет України
«Київський політехнічний інститут імені Ігоря Сікорського»
ORCID: 0000-0002-6665-2744

ОЦІНКА РОЗМІРНИХ ХАРАКТЕРИСТИК НАНОЧАСТИНОК ФОТОКАТАЛІЗАТОРІВ НА ОСНОВІ ОКСИД/ГІДРОКСИДУ МАНГАНУ

Оскільки розмір є ключовою характеристикою, що визначає приналежність матеріалу до класу наноматеріалів, його точна оцінка має критичне значення. Крім того, розмір наночастинок (НЧ) впливає на ефективність матеріалу для каталітичних і фотокаталітичних застосувань. Було синтезовано та охарактеризовано низку композиційних матеріалів, що складаються із оксид/гідроксидних сполук мангану з нанотрубками галуазиту, приділяючи особливу увагу параметрам розміру наночастинок, критичних для функціонального застосування. Кілька аналітичних методів, включаючи трансмісійну та скануючу електронну мікроскопію (TEM/SEM) у поєднанні з програмним забезпеченням IMAGJ, динамічне розсіювання світла (DLS) і рентгенівську дифракцію (XRD), використовувалися для оцінки розмірів НЧ. Зразки хімічно синтезували при температурі навколишнього середовища 15–20°C з розчину $MnSO_4$ за участю окисника H_2O_2 при контролі pH на рівні 6, 10. Напівширина розподілу за розміром була визначена як ключовий фактор при оцінці помилки, пов'язаної з ефектами розміру в наноматеріалах. Показано, що відносна похибка щодо навіть критичного для квантових ефектів розміру 100 нм становить приблизно 10% для хімічно синтезованих зразків та приблизно 20% для MnO_2 Придніпровського хімічного заводу (Україна). Ці значення похибок достатньо великі для кількісних оцінок і підкреслюють потребу в покращеному контролі розподілу за розміром за допомогою оптимізованих умов синтезу, зокрема температури. Крім того, у той час як XRD в основному відображає розміри кристалітів, часто менші за фактичні розміри наночастинок, які спостерігаються за допомогою TEM/SEM, DLS має тенденцію завищувати розміри через агломерацію частинок. Дані щодо розміру частинок досліджуваних зразків, отримані методом Рітвельда, добре узгоджуються із результатами оцінки в програмному забезпеченні IMAGJ для окремих випадків хімічно синтезованих зразків, взятих для аналізу. Комплексна характеристика зразків підкреслює їхній потенціал для майбутніх нанозастосувань, забезпечуючи основу для подальших досліджень і розробок.

Ключові слова: *наночастинка, розмір, оцінка, оксиди/гідроксиди мангану, фотокаталіз.*

Formulation of the problem

The growing need for modern electronics and other high-tech industries creates constant demand for new and improved materials and technologies. The miniaturisation trend in aforementioned areas during the last decades becomes a peculiar response toward the famous R. Feynman Nobel Prize lecture "There's Plenty of Room at the Bottom: An Invitation to Enter a New Field of Physics" formulating ability to manipulate matter on an atomic or nanoscale [1]. The quintessence of this tendency is the intensive development of nanotechnologies, which is concentrated on quantum-scale size effects that arise at particle sizes of about 10–100 nm.

Traditional synthetic procedures for many materials, including oxides, should be revised in order to meet modern requirements. It is well-known that oxides of transition metals have found wide practical applications. The evaluation of approaching existing synthesis methods of these oxides toward nanotechnology needs is subjected to numerous in-depth studies.

Manganese dioxide is a cheap and widely distributed natural material. It is characterised by structural diversity and, as a result, unique properties. That is why it is widely used as an electrode material in batteries [2–4], a catalyst of oxidation processes [5], and a photocatalyst in water treatment [6]. The functional properties of non-stoichiometric oxides directly depend on the material particles' origin, morphology, dispersion, shape, and size. Therefore, it is essential to control these parameters when synthesising new materials.

According to European Commission recommendations, a nanomaterial is a natural, incidental, or manufactured material containing particles in an unbound state or as an aggregate or agglomerate, and where 50% or more of the particles in the number size distribution have one or more external dimensions in the size range 1 nm – 100 nm [7]. Since "nanomaterial" is defined by particle size, measuring the size distribution of products is essential to confirm whether they meet these parameters. However, due to technical challenges, there has been a growing discussion aimed at identifying practical solutions for accurately measuring size distribution [8]. Transmission electron microscopy (TEM) is considered a promising technique for measuring the size distribution of nanomaterials. In addition to detailed morphological observations, TEM provides the necessary information for particle size distribution.

Analysis of recent research and publications

Manganese dioxide has found applications in batteries more than a century ago [9,10]. Manganese oxide compounds with versatility of structure behaviour have practically important oxidising agent, catalytic, and electrocatalytic properties [11, 12]. Recent studies revealed their potential as a photocatalyst [13], including the water-splitting process.

By combining semiconductive nanoparticles of MnO2 with C3N4, active composite photocatalysts of water-splitting Hydrogen Evolving Reaction (HER) were prepared [14,15]. MnOOH is an oxyhydroxide of Mn(III)-state. It exists in 3 crystalline polymorphs: α -groutite, β -feitknechtite and γ-manganite. It found wide use as chemical catalysts, molecular sieves, and cathode materials in primary and rechargeable batteries [16].

Numerous studies have explored the effectiveness of hausmannite in the photodegradation of various dyes, including Alizarin Yellow, Methylene Blue, and Methyl Orange. It is reported as an excellent sensor material for identifying volatile organic compounds [17]. Furthermore, it is a significant energy storage medium, particularly as an anode material for lithium-ion batteries [18]. Additionally, its role as an efficient catalyst [13] in a wide range of oxidation and reduction reactions underscores its importance in catalysis.

The advantages of applying nanomaterials in photocatalysis include the shorter electron-hole pair path and lower this pair recombination probability [19].

Formulation of the purpose of the research

Thus, this study aim is to test the opportunities of modern software, namely IMAGJ and QTIPLOT, in evaluating nanodimensional characteristics of obtained materials to study further functionality size effects.

Presentation of the main research material

Synthetic procedures. Powder samples of manganese oxide materials were obtained by chemical deposition methods. A typical chemical synthesis of oxide materials was as follows: dissolution of 13.85 g of $MnSO_4 \cdot 5H_2O$ in 100 ml of water, adding $(NH_4)_2SO_4$ to achieve a ratio of ions Mn^{2+} : NH_4^+ equal 1:2 for samples 2 and 6. Halloysite nanotubes (HNTs) of 1 g for samples 1, 2, 6, and 7 were also added (Table 1). For samples with HNTs, 1 hour of vacuuming was applied to achieve complete removal of air and fill the lumen with a solution. pH was adjusted through the addition of ammonium hydroxide. Hydrogen peroxide was added dropwise as an oxidant while maintaining continuous mechanical stirring. The product was centrifuged, washed with distilled water and dried at 160°C until constant mass. Samples considered as a standard were also used (MnO_2, Pridneprovsky Chemical Plant (PCP), Kamianske and HNTs, Sigma Aldrich).

Characterization methods. ζ-potential and Dynamic light scattering analysis (DLS). ζ-potential and dynamic light scattering measurements were performed in 0.001 mass % aqueous dispersions by a Zetasizer NANO-ZS (Malvern Instruments) at 25 ± 0.1°C. For ζ-Potential experiments, a disposable folded capillary cell was used. Analysis of the intensity of scattered light made it possible to obtain data on the hydrodynamic diameter of the particles and their ζ-potential. These results provided a description of the particle sizes and surface charge properties.

The characterization of samples also included: thermogravimetry (Thermogravimetric Analyzer Discovery TGA550 with TRIOS Software); energy-dispersive X-ray fluorescence (mobile precision analyzer Olympus Innov-X DS-2000 Delta);

X-ray diffraction method (X-ray diffractometer Rigaku, MiniFlex600 with a CuKα radiation source); FTIR spectroscopy was performed on PerkinElmer Spectrometer Frontier. The composite sample was mixed with KBr in 1 : 100 ratio and pressed into tablets that had a grayish-brown color. Spectra were registered in the range of 400–4000 cm^{-1}.

Table 1

Samples and their synthesis conditions

Sample name	Sample composition	HNTs content, g	1.5M NH_4^+	pH
CS-1	Mn-HNT-pH10-H_2O_2	1		10
CS-2	Mn-NH_4^+-HNT-pH10-H_2O_2	1	+	10
CS-3	Mn-NH_4^+-pH10		+	10
CS-4	Mn-NH_4^+-pH5-6-H_2O_2		+	5-6
CS-5	Mn-pH5-6-H_2O_2			5-6
CS-6	Mn-NH_4^+-HNT-pH5-7.5-H_2O_2	1	+	5-7.5
CS-7	Mn-HNT-pH5-6-H_2O_2	1		5-6
CS-8	Mn-NH_4^+-HNT-pH5-7.5-H_2O_2slow (72h)		+	5-7.5
CS-9	Mn-NH_4^+-HNT-pH5-8-H_2O_2 express (2h)		+	5-8

To determine the size of nanoparticles, the following procedure was used: high-quality microscope images from Scanning Electron Microscopy (SEM, Tescan, Czechia) or Transmission Electron Microscopy (TEM, JEM 1200-EX, JEOL, Japan) were used to perform at least 60 measurements of the diameter, length in the case of anisotropic nanoparticles (NP), and the sizes of aggregates by means of the ImageJ software (Fig. 1).

Results and Discussion. Synthesized samples after washing, drying, and grinding were fine powders from beige to black colour. The yield of products has varied between low and relatively high depending on the presence of HNTs. For instance, the yield of samples synthesized without HNTs was minimal (to within 2–30% by mass) and was 50–65% by mass at the same conditions with HNTs. To address the objectives of this study, a subset of samples from the series listed in Table 1 was selected for further analysis, as shown in Table 2.

Qualitative XRD phase analysis of prospective phase candidates included comparing their main reflexes with diffraction databases of XRD patterns using PDF-2 database of the International Centre for Diffraction Data (PCPDFWIN version 2.0, ICDD, 1998), Match 2.0, and Profex Version 5.2.5. The phase composition of Samples CS1-CS9 was complex and included Mn_3O_4 at pH=10 and MnOOH/MnO_2 at pH about 6 as the main components. The peaks of HNTs were also identified.

TEM studies were performed to reveal the morphology, size, and dimensions of the obtained NPs. Powdered samples were subjected to preliminary ultrasound processing for several minutes in the aqueous medium to improve the visibility of NPs. Some typical TEM images are shown in Fig. 2.

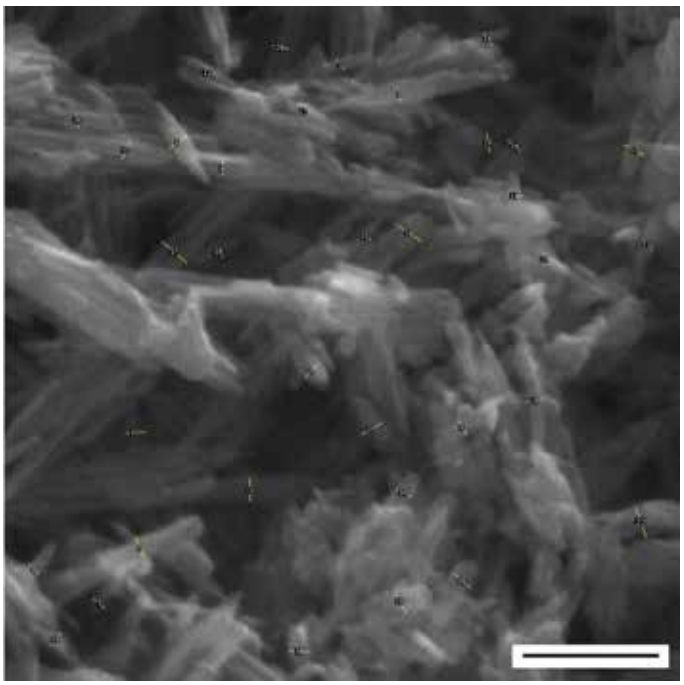

Fig. 1. SEM image of PCP MnO_2 (standard) with measurements performed on nanoparticles shown by marks. The scale bar corresponds to 200 nm

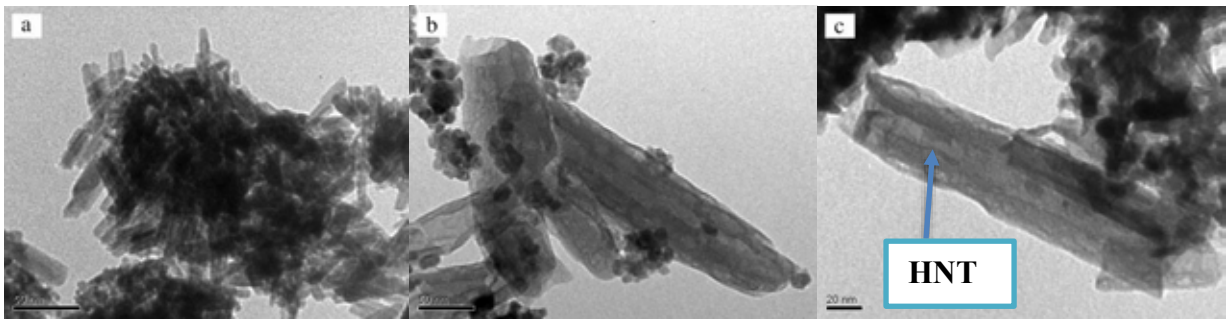

Fig. 2. TEM images of Samples: CS-5 of manganese oxide/hydroxide (a), and heterostructures with HNTs of CS-1 (b) and CS-6 (c)

The first observation that can be made is related to the manganese oxide/hydroxide morphology dependence on pH: elongated NPs forming agglomerates are typical for pH close to 6, and very tiny and small shapeless NPs were observed at pH = 10. The decoration effect of HNTs by oxide/hydroxide NPs can be visible in Fig. 2(b). The HNT's lumens in Fig. 2 b, c are not filled with oxide/hydroxide NPs.

ImageJ software was applied to evaluate the parameters of NPs in Samples (Fig. 3). Statistical processing of the obtained results was carried out using the Qtiplot program, and it was established that the diameter of the nanoparticles of the synthesized sample is, on average, half that of the PCP, and the sizes of the nanoparticles fluctuate in a much smaller range. The average particle size is 10.4–15.2 nm (78% of measurements fall into this range). The PCP sample' average size is between 26 and 34 nm (for 70% of measurements), Table 2.

Table 2

Evaluated parameters of NPs from the Gaussian peak

Sample name	Averaged size of NPs / nm	Maximum of distribution curve, size / nm	Distribution curve width at half-height / nm
MnO_2 PCP	27.84±8.19	22.85±0.8	19.23
CS-1. Mn-HNT-pH10-H_2O_2	14.96±5.64	11.69±0.38	9.89
CS-2. Mn-NH_4-HNT-pH10-H_2O_2	12.11±6.35	7.57±0.2	9.89
CS-5. Mn-pH5-6-H_2O_2	10.79±3.62	8.68±0.19	9.89
CS-6. Mn-NH_4-HNT-pH5-7.5-H_2O_2	10.89±4.84	6.92±0.45	7.14
CS-7. Mn-HNT-pH5-6-H_2O_2	14.45±5.06	11.67±0.12	9.89

The distribution curve width at its half-height is an important characteristic of a nanomaterial for studying the size effects of functionality, including photocatalytic activity. It describes the distribution of NPs around the average value of size. This parameter shown in Table 2 is practically identical for samples obtained by one method and independent of the presence of HNTs. The narrowest distribution demonstrates Sample 6. The widest distribution has MnO_2 PCP Sample (19.23 nm). The smallest average size have manganese oxide/hydroxide NPs in Sample 6, and the maximal size display MnO_2 PCP NPs.

It can be seen that data of columns 1 and 2 in Table 2 differ by 20–50%. At the same width of the distribution curve at its half-height it is preferable to operate by the maximum of the distribution curve versus the average value of NP's size. Even at some scattered values, distribution curve analysis shows the most useful information to evaluate applicability of data to study size effects in nanomaterials.

DLS method demonstrates the tendency to NPs agglomeration (Table 3). As it was expected, the maximal tendency to form aggregates demonstrates MnO_2 PCP Sample. In general, average size data obtained by DLS method by about 10 times larger than the data of direct measurements processed by IMAGJ software. ζ-potential values in Table 3 and of pure HNTs (-30 mV in the pH range from 2 to 8 [20]) confirm the incipient instability of NPs of Samples.

The data of Rietveld refinement of the Samples performed by Powder Cell v.2.3 software were also used to evaluate the sizes of coherent scattering regions(CSR). It can be concluded that results are in agreement with data in Table 2 for main phase components such as Mn_3O_4 and MnOOH. On the other hand, XRD diffraction patterns of all Samples demonstrate amorphous galo and low values of the signal/noise ratio. These obstacles were taken into account by subtracting an amorphous background when possible. Evaluations by modelling of semiamorphous phase components contributing XRD patterns resulted in lower CSR sizes to within 4–6 nm.

The specific surface area of the PCP sample, as determined by the BET method, is 22 m^2/g, whereas the chemically synthesized samples exhibit significantly higher values, ranging from 50 to 70 m^2/g. From this, we can conclude that the PCP sample has a high degree of aggregation, which is confirmed by visual observations.

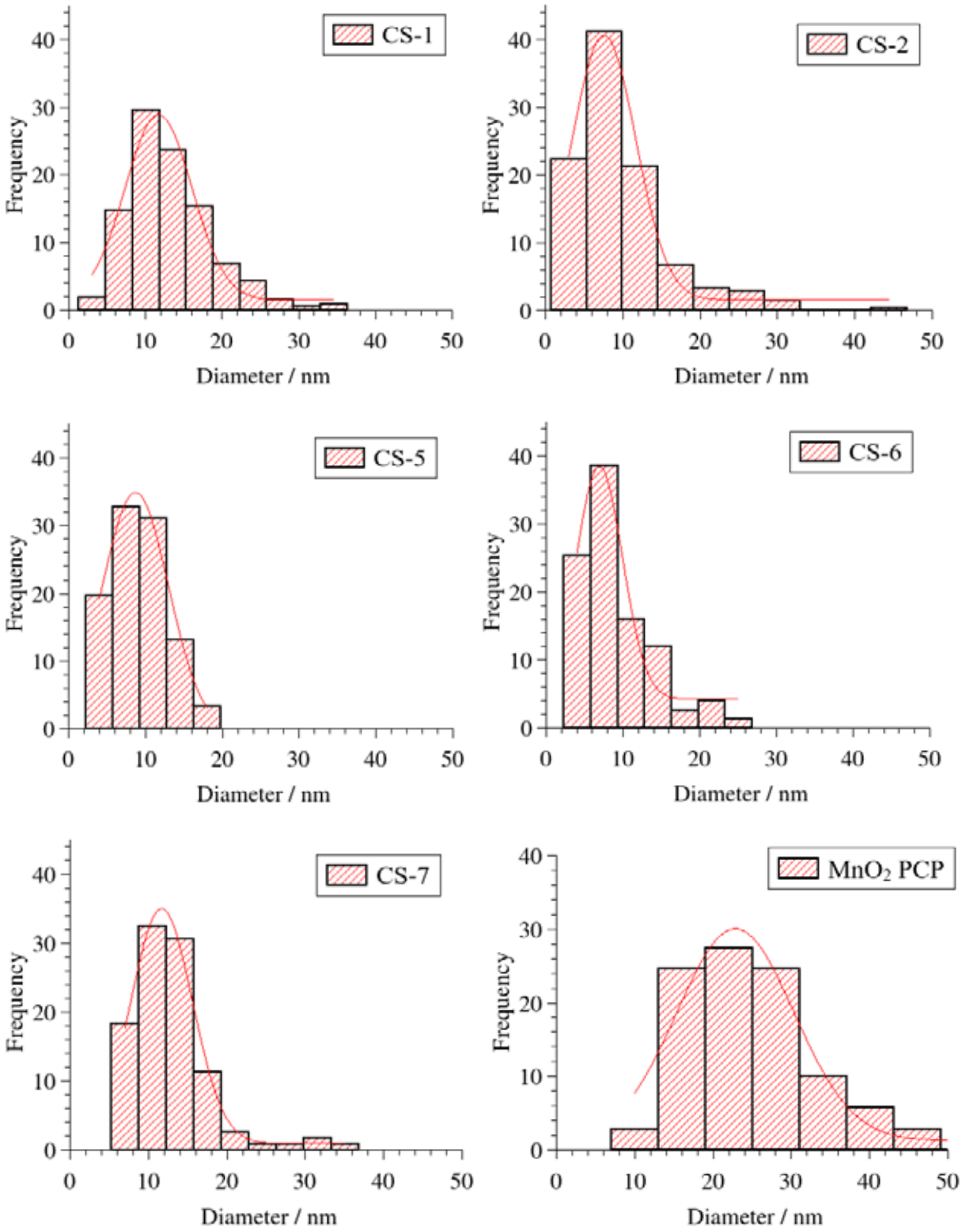

Fig. 3. The dependence of the percentage of appearance on the nanoparticle size is shown for the synthesised samples and PCP MnO_2

Table 3

Data obtained using DLS

Sample name	Average size / nm	ζ-potential / mV
MnO_2 PCP	222.447±83.21	-21.97±0.85
CS-1. Mn-HNT-pH10-H2O2	119.08±48.68	-18.10±0.56
CS-2. Mn-NH4-HNT-pH10-H2O2	141.16±43.05	-16.13±0.90
CS-5. Mn-pH5-6-H2O2	175.44±86.19	-19,2±1.11
CS-6. Mn-NH4-HNT-pH5-7.5-H2O2	143.02±52.38	-19.4±1.7
CS-7. Mn-HNT-pH5-6-H2O2	118.2±36.08	-15.8±0.75

Conclusions

The series of chemically deposited composites of oxide/hydroxide compounds of manganese with halloysite nanotubes was synthesized. The characterisation of them was made focused on the parameters related closely to NPs. Bearing in mind the aim to study size effects in further experiments with such functional applications as catalysis and photocatalysis, the evaluations of sizes of nanoparticles were made by available methods of TEM/SEM combined with IMAGJ software, DLS, and XRD. Direct measurements of NPs' morphology parameters have advantages over classical methods such as XRD, DLS, etc. IMAGJ software represents a suitable user interface for SEM/TEM image analysis and supplies a researcher with valuable information not equivalent to the results of the other aforementioned methods.

The obtained results of size distribution half-width are the suitable measure of size effect evaluation error in nanomaterials. It can be seen that the relative error towards even critical for quantum effects revealing size of 100 nm makes up about 10% for Samples CS1-9 and about 20% for MnO_2 PCP. These error values are large enough for quantitative evaluations. Therefore, the size distribution half-width needs further control by synthetic or other procedures. The most prospective parameter for optimisation in this case could be temperature of chemical deposition since our experiment maintained at constant ambient temperature of approximately 15–20°C. As we know, XRD signal broadening shows the sizes of coherent scattering regions or crystallites that are generally less and not equal to the actual sizes of NPs that can be seen in SEM/TEM images. On the contrary, average sizes of NPs received from the DLS method are usually larger than true sizes since NPs' agglomeration occurs. It can be concluded from performed analysis of NPs sizes data of studied Samples that the exact method of Rietveld refinement resulted in good agreement with IMAGJ software for particular cases of Samples CS1-9 taken for analysis. It is also clear that all information from characterisation of Samples is valuable for further nanoapplications.

Acknowledgements

Authors thank to the European Union for funding of this study within H-GREEN project "Innovative Functional Oxide Materials for Green Hydrogen Energy Production (HORIZON-TMA-MSCA-SE action).

References

1. Feynman, R. P. (2011). There's plenty of room at the bottom: An invitation to enter a new field of physics. *Resonance*, *16*(9), 890–905. https://doi.org/10.1007/s12045-011-0109-x

2. Cheng, F., Zhao, J., Song, W., Li, C., Ma, H., Chen, J., & Shen, P. (2006). Facile Controlled Synthesis of MnO2 Nanostructures of Novel Shapes and Their Application in Batteries. *Inorganic Chemistry*, *45*(5), 2038–2044. https://doi.org/10.1021/ic051715b

3. Liu, X., Chen, C., Zhao, Y., & Jia, B. (2013). A Review on the Synthesis of Manganese Oxide Nanomaterials and Their Applications on Lithium-Ion Batteries. *Journal of Nanomaterials*, *2013*(1), 736375. https://doi.org/10.1155/2013/736375

4. Dose, W., Sharma, N., Webster, N., Peterson, V., & Donne, S. (2014). Kinetics of the Thermally-Induced Structural Rearrangement of γ-MnO 2. *The Journal of Physical Chemistry C*, *118*, 24257–24265. https://doi.org/10.1021/jp506914j

5. Qi, L., Liu, Y., Tang, Y., Jiang, X., Xie, F., Wan, L., Wang, Z., Wang, X., & Lü, C. (2024). Highly coupled MnO2/Mn5O8 Z-scheme heterojunction modified by Co3O4 co-catalyst: An efficient and stable photocatalyst to decompose gaseous benzene. *Applied Catalysis B: Environment and Energy*, *353*, 124099. https://doi.org/10.1016/j.apcatb.2024.124099

6. Yang, R., Fan, Y., Ye, R., Tang, Y., Cao, X., Yin, Z., & Zeng, Z. (2021). MnO2-Based Materials for Environmental Applications. *Advanced Materials*, *33*. https://doi.org/10.1002/adma.202004862

7. European Commission. (2011). *Commission Recommendation of 18 October 2011 on the definition of nanomaterial Text with EEA relevance*. *Off. J. Eur. Union*(L275),38–40. https://eur-lex.europa.eu/LexUriServ/LexUriServ.do?uri=OJ:L:2011:275:0038:0040:EN:PDF

8. Kumagai, K. (2015). Optimization of Image Contrast for Size Distribution Measurements of Nanomaterials by Transmission Electron Microscopies Including TEM and T-SEM. *Metallography, Microstructure, and Analysis*, *4*(6), 475–480. https://doi.org/10.1007/s13632-015-0237-x

9. Desai, B. D., Fernandes, J. B., & Dalal, V. N. K. (1985). Manganese dioxide–A review of a battery chemical Part II. Solid state and electrochemical properties of manganese dioxides. *Journal of Power Sources*, *16*(1), 1–43. https://doi.org /10.1016/0378-7753(85)80001-X

10. Tang, Y., Zheng, S., Xu, Y., Xiao, X., Xue, H., & Pang, H. (2018). Advanced batteries based on manganese dioxide and its composites. *Energy Storage Materials*, *12*, 284–309. https://doi.org/10.1016/j.ensm.2018.02.010

11. Yunxuan, Z., Chang, C., Teng, F., Zhao, Y., Chen, G., Shi, R., Waterhouse, G., Huang, W., & Zhang, T. (2017). Defect-Engineered Ultrathin δ-MnO2 Nanosheet Arrays as Bifunctional Electrodes for Efficient Overall Water Splitting. *Advanced Energy Materials*, *2017*. https://doi.org/10.1002/aenm.201700005

12. Meng, Y., Song, W., Huang, H., Ren, Z., Chen, S.-Y., & Suib, S. L. (2014). Structure–Property Relationship of Bifunctional MnO2 Nanostructures: Highly Efficient, Ultra-Stable Electrochemical Water Oxidation and Oxygen Reduction Reaction Catalysts Identified in Alkaline Media. *Journal of the American Chemical Society*, *136*(32), 11452–11464. https://doi.org/10.1021/ja505186m

13. Li, N., He, M., Lu, X., Liang, L., Li, R., Yan, B., & Chen, G. (2021). Enhanced norfloxacin degradation by visible-light-driven Mn3O4/γ-MnOOH photocatalysis under weak magnetic field. *Science of The Total Environment*, *761*, 143268. https://doi.org/10.1016/j.scitotenv.2020.143268

14. Wang, N., Li, J., Wu, L., Li, X., & Shu, J. (2016). MnO2 and carbon nanotube co-modified C3N4 composite catalyst for enhanced water splitting activity under visible light irradiation. *International Journal of Hydrogen Energy*, *41*(48), 22743–22750. https://doi.org/10.1016/j.ijhydene.2016.10.068

15. Li, X., Fang, G., Qian, X., & Tian, Q. (2022). Z-scheme heterojunction of low conduction band potential MnO2 and biochar-based g-C3N4 for efficient formaldehyde degradation. *Chemical Engineering Journal*, *428*, 131052. https:// doi.org/10.1016/j.cej.2021.131052

16. Crisostomo, V. M. B., Ngala, J. K., Alia, S., Dobley, A., Morein, C., Chen, C.-H., Shen, X., & Suib, S. L. (2007). New Synthetic Route, Characterization, and Electrocatalytic Activity of Nanosized Manganite. *Chemistry of Materials*, *19*(7), 1832–1839. https://doi.org/10.1021/cm062871z

17. Bai, Z., Sun, B., Fan, N., Ju, Z., Li, M., Xu, L., & Qian, Y. (2012). Branched Mesoporous Mn3O4 Nanorods: Facile Synthesis and Catalysis in the Degradation of Methylene Blue. *Chemistry – A European Journal*, *18*(17), 5319–5324. https://doi.org/10.1002/chem.201102944

18. Kong, Y., Jiao, R., Zeng, S., Cui, C., Li, H., Xu, S., & Wang, L. (2020). Study on the Synthesis of Mn3O4 Nanooctahedrons and Their Performance for Lithium Ion Batteries. *Nanomaterials*, *10*(2), 367. https://doi.org/10.3390/ nano10020367

19. Nakade, S., Saito, Y., Kubo, W., Kitamura, T., Wada, Y., & Yanagida, S. (2003). Influence of TiO_2 Nanoparticle Size on Electron Diffusion and Recombination in Dye-Sensitized TiO_2 Solar Cells. *The Journal of Physical Chemistry B*, *107*(33), 8607–8611. https://doi.org/10.1021/jp034773w

20. Abdullayev, E., & Lvov, Y. (2013). Halloysite clay nanotubes as a ceramic “skeleton” for functional biopolymer composites with sustained drug release. *Journal of Materials Chemistry B*, *1*(23), 2894. https://doi.org/10.1039/c3tb20059k